Liquid Crystals
Publication details, including instructions for authors and subscription information:
http://www.informaworld.com/smpp/title~content=t713926090

SmA-SmC-B_2 polymorphism in an achiral cyano substituted banana-shaped mesogen

W. Weissflog; L. Kovalenko; I. Wirth; S. Diele; G. Pelzl; H. Schmalfuss; H. Kresse

To cite this Article Weissflog, W. , Kovalenko, L. , Wirth, I. , Diele, S. , Pelzl, G. , Schmalfuss, H. and Kresse, H.(2000) 'SmA-SmC-B_2 polymorphism in an achiral cyano substituted banana-shaped mesogen', Liquid Crystals, 27: 5, 677 — 681
To link to this Article: DOI: 10.1080/026782900202543
URL: http://dx.doi.org/10.1080/026782900202543

LIQUID CRYSTALS, 2000, VOL. 27, NO. 5, 677–681

Preliminary communication

SmA–SmC–B_2 polymorphism in an achiral cyano substituted banana-shaped mesogen

W. WEISSFLOG,* L. KOVALENKO, I. WIRTH, S. DIELE, G. PELZL,
H. SCHMALFUSS and H. KRESSE

Institut für Physikalische Chemie, Martin-Luther-Universität Halle-Wittenberg,
Mühlpforte 1, 06108 Halle/S., Germany

(*Received 12 November 1999; accepted 26 January 2000*)

A new achiral five-ring banana-shaped mesogen is presented which has a cyano substituent in the 4-position of the central core. Microscopical, X-ray, dielectric and electro-optical investigations give evidence for the unusual phase sequence B_2, SmC, SmA. The B_2 phase shows an antiferroelectric switching behaviour; the spontaneous polarization was found to be 330 $nC\,cm^{-2}$.

In 1996 Niori *et al.* [1] reported a new ferroelectric phase formed by achiral banana-shaped mesogens. In the intervening period, a number of new banana-shaped mesogens have been synthesized [2–14]. Up to now five smectic-like mesophases without in-plane order have been clearly distinguished by X-ray diffraction measurements [2, 15] and three of them show antiferroelectric switching behaviour. The phase behaviour of banana-shaped mesogens is determined by different structural elements—by the size of the molecule, the position as well as the magnitude of the bend, the number and position of substituents, the linkage groups and the length and structure of the terminal chains. Generally it is found that minor changes in these structural elements can lead to drastic changes in the phase behaviour. For example, the liquid crystalline properties can be strongly influenced by the nature and position of substituents at the central core.

Starting from the basic molecule of the parent series reported by Niori *et al.* [1] a CH_3-substituent in the 2-position gives rise to the formation of the switchable B_2 and B_5 phases [5]. By introduction of a nitro group in the 2-position, a B_7 and a higher ordered, low temperature phase arise [6]. The introduction of chlorine in the 4-position gives a B_2 phase as in the unsubstituted compounds [7, 8]. Even small substituents in the 5-position (that means at the top of the bent molecule) are disadvantageous for the formation of mesophases. Therefore, for the 5-cyano substituted compounds, liquid crystalline properties could not be detected. In this paper we present a banana-shaped mesogen where a cyano group is substituted in the 4-position of the central core.

The synthetic route is shown in the following reaction scheme:

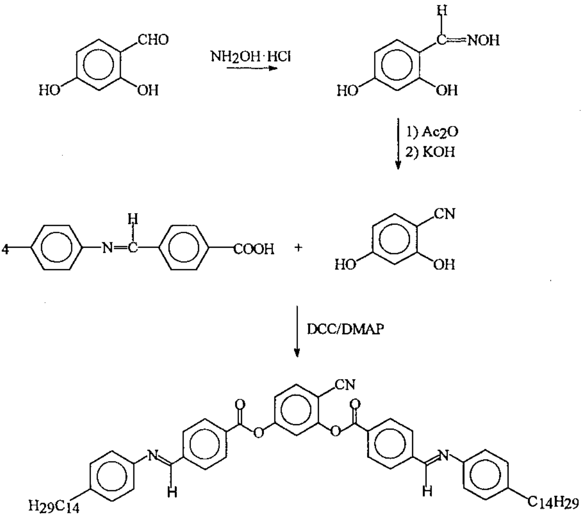

The elimination of water from 2,4-dihydroxybenzaldoxime prepared from 2,4-dihydroxybenzaldehyde was brought about according to a slightly modified procedure of Serrano *et al.* [16, 17] with acetic anhydride, and following deprotection of the acetate gave 2,4-dihydroxybenzonitrile. The esterification of 4-(4-tetradecylphenyliminomethyl)benzoic acid [18] was successful using DCC/DMAP. Experimental details will be given elsewhere.

---

*Author for correspondence.

Liquid Crystals ISSN 0267-8292 print/ISSN 1366-5855 online © 2000 Taylor & Francis Ltd
http://www.tandf.co.uk/journals

An initial identification of the liquid crystalline phases was carried out using polarizing optical microscopy (Leitz Orthoplan equipped with a Linkam THM 600/S hot stage). The phase transition temperatures were detected by differential scanning calorimetry (DSC7, Perkin Elmer). The phase structures were determined using X-ray diffraction on powder-like samples. X-ray scattering experiments on powder-like samples were carried out using the Guinier method (Huber Diffraktionstechnik GmbH) and small angle equipment. In all X-ray experiments, the temperature was controlled to better than ± 1 K. Electro-optical investigations were made using the usual experimental set-up described in an earlier paper [7]. Dielectric measurements were carried out on non-oriented samples in a brass capacitor (spacing 0.01 cm) coated with gold. The cell was calibrated with cyclohexane. Capacity and resistance were measured in the frequency range between 0.1 Hz and 10 MHz using a Solartron-Schlumberger impedance analyser in combination with a Chelsea interface. The temperature was controlled by a Eurotherm control unit.

Three mesophases could be clearly distinguished by their characteristic textures. The high temperature phase exhibits a fan-shaped texture, figure 1 (*a*), or a homeotropic texture indicating a SmA phase. On cooling, the fan-shaped texture is transformed into a broken fan-shaped texture, figure 1 (*b*), whereas the homeotropic texture forms a schlieren texture. In consequence this phase is assigned as a SmC phase. The transition into the low temperature phase is accompanied by a clear change of the broken fan-shaped texture, figure 1 (*c*), and by a discontinuous change of the birefringence in the SmC schlieren texture. Taking into consideration the results of the calorimetric measurements, the following transition scheme results where the assignment of the low temperature phase is based on the results of electro-optical and dielectric measurements.

$$\begin{array}{lllllllllll} \text{Cr} & 88 & \text{B}_2 & 126 & \text{SmC} & 140 & \text{SmA} & 164.5 & \text{I} & & (^\circ\text{C}) \\ & [20.4] & & [1.5] & & [\text{-}] & & [6.6] & & & (\text{kJ mol}^{-1}) \end{array}$$

Note that at the transition SmA–SmC there is no calorimetric peak, indicating a phase transition of second order, while for the transition of the SmC phase into the low temperature phase a transition enthalpy of 1.5 kJ mol^{-1} was measured. In comparison with the analogous chloro substituted compound (Cr 68 B$_2$ 127 I [7]) a much higher clearing temperature occurs.

In electro-optical measurements the SmC phase shows a weak field-induced switching whereby the textures in the switched state are independent of the sign of the applied field. Since the same switching behaviour was also observed with an a.c. field up to 10 kHz, we explain this by a dielectric reorientation caused by the coupling of the field with the dielectric anisotropy of the SmC phase. The switching behaviour is completely changed at the transition into the low temperature phase. Applying an electric field in the fan-shaped texture, irregular stripes parallel to the smectic layers arise which is characteristic for a B$_2$ phase. It is seen from figure 2 that the texture of the switched state is different for an opposite sign of the applied field. Applying a triangular voltage, two current peaks appear indicating an antiferroelectric switching behaviour (figure 3). From the current response, a spontaneous polarization of 330 nC cm^{-2} could be determined, which increases slightly with falling temperature.

Dielectric measurements were made during cooling to reduce the time for temperature stabilization of the sample. Nevertheless, decomposition of the sample was observed, resulting in a shift of the phase transition temperatures. The samples could not be oriented. The dielectric loss ε'' and dielectric constant ε' were calculated at different frequencies. Figure 4 shows dielectric dispersion curves for the three mesophases over a limited frequency range. The high ε' values at low frequencies result from the formation of a double layer at the interface between the gold and the liquid crystal. In the isotropic (I) and smectic A (SmA) phases, the expected dielectric constants of 5 and 8, respectively, at 10 kHz were obtained. The decrease of the dielectric constants at higher frequencies results from dielectric dispersion connected with the reorientation of the molecules about their long axes [7]. The ε' values in the SmC phase of about 16 are unusually high. In the B$_2$ phase an additional low frequency relaxation process at about 100 Hz is detected.

For a detailed analysis, both the (imaginary) dispersion and (real) absorption curves at a given temperature were fitted together to one or two (B$_2$) Cole–Cole mechanisms taking into consideration the (imaginary) conductivity and the real double layer [7]. The limits of the dielectric constants so obtained are presented in figure 5. Stepwise changes of the dielectric constants indicating a phase transition are marked by arrows and vertical lines for the temperature shifts of the phase transitions. The respective relaxation times are given in figure 6. By comparison with analogous substances it is evident that the observed relaxation is related to the reorientation of the molecules about their long axes.

In figure 5 the clear decrease of all phase transition temperatures (marked by vertical arrows) is caused by partial decomposition of the substance at the high temperatures. The static dieletric constant ε_0 in the isotropic state behaves as normal, and that in the SmA phase can be explained by a more planar orientation of the molecules with a high perpendicular dipole moment. The relaxation time for the reorientation of the molecules about the molecular long axes does not change at the phase transition as usually observed in calamitic liquid

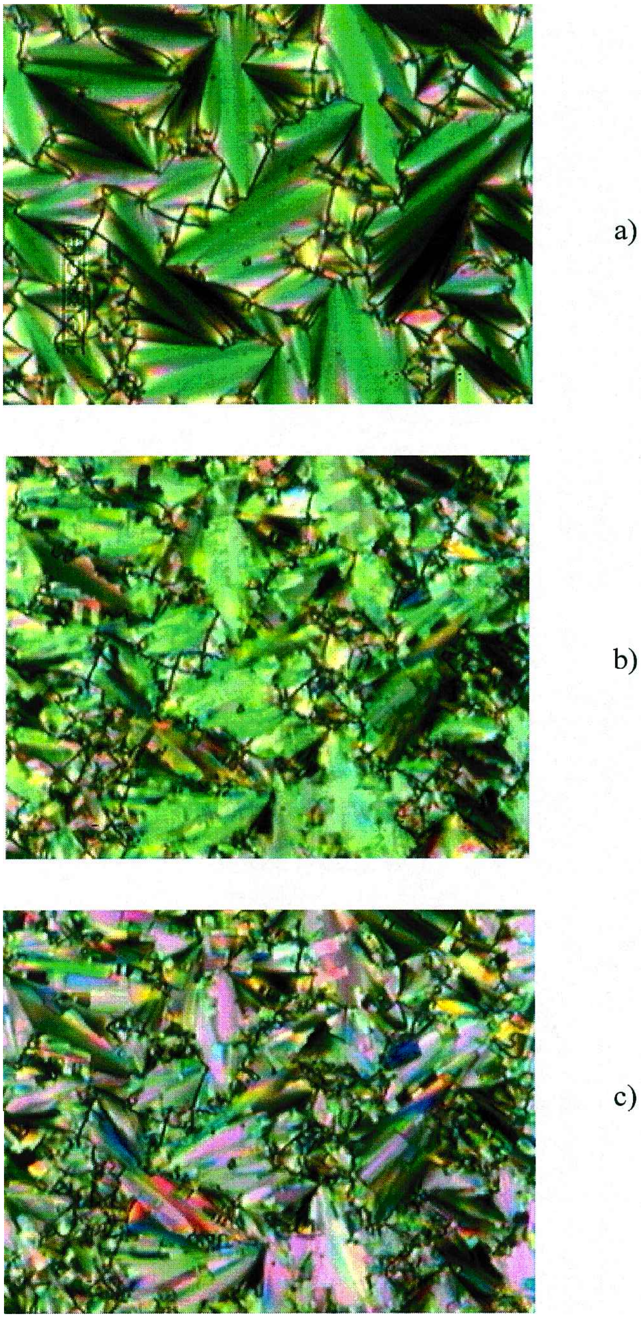

Figure 1. (*a*) Fan-shaped texture of the SmA phase (142°C); (*b*) broken fan-shaped texture of the SmC phase (128°C); (*c*) broken fan-shaped texture of the B_2 phase (125°C).

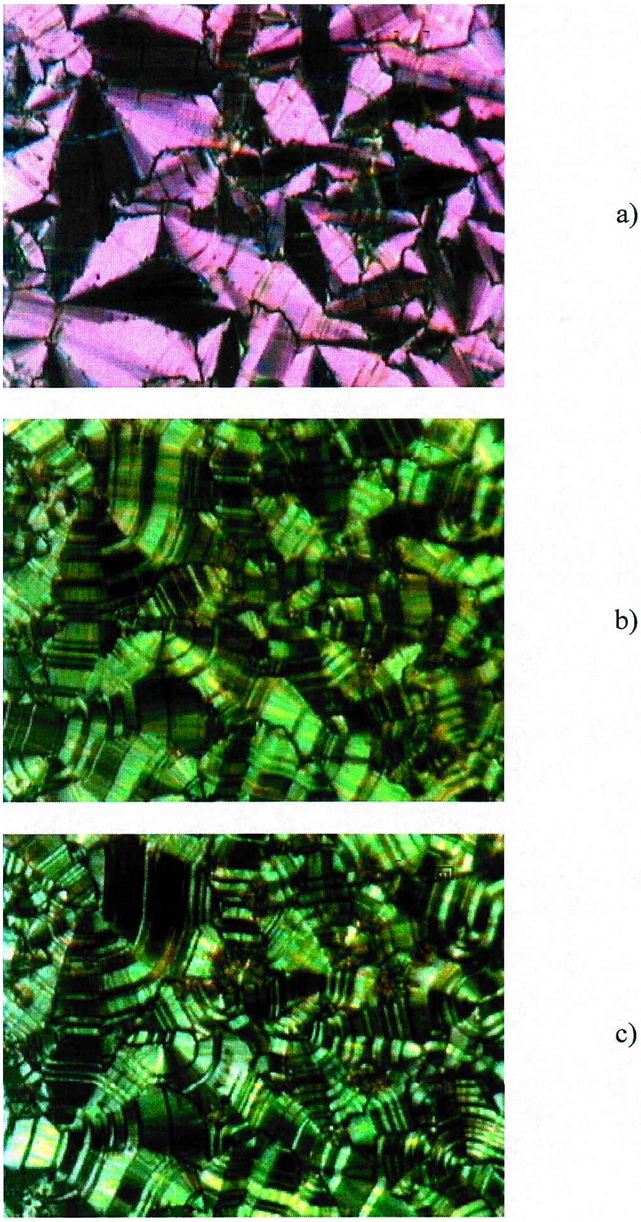

Figure 2. Texture of the B_2 phase: (*a*) 0 V; (*b*) +42 V; (*c*) − 42 V. Sample thickness = 10 μm; temperature = 110°C.

crystals [18]. Quite unexpected results are obtained in the SmC state: dielectric constants and relaxation frequencies increase with decreasing temperature. In this way ε_0 increases to the exotic value of about 30 which can never result from any independent dynamic effect of the dipolar molecules. So, we have to assume in the SmC phase a gradual change of the structure to one with increasing positive dipole correlation. In this way the observed SmC phase may be a transition state into the B_2 phase where such effects are observed in all substances investigated [7, 19, 20]. Such a behaviour is also seen in the relaxation times. Instead of the expected step of the relaxation times, a continuous increase of τ_2 is observed. The B_2 phase shows the typical two absorption ranges (see also figure 4). By cooling below 97°C further anomalies are seen in figure 4 which may result from an additional phase transition. The dynamic and calorimetric investigations do not reflect this anomaly.

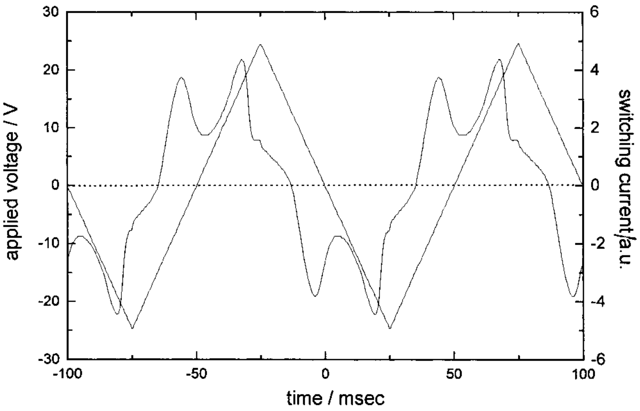

Figure 3. Switching current response in the B_2 phase obtained by applying a triangular voltage (50 V_{pp}; 10 Hz; 90°C; sample thickness 6 μm).

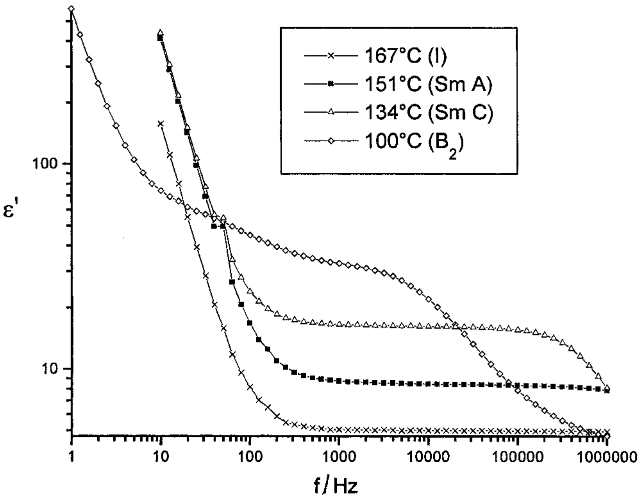

Figure 4. Dielectric dispersion curves of different phases (I, SmA, SmC, B_2).

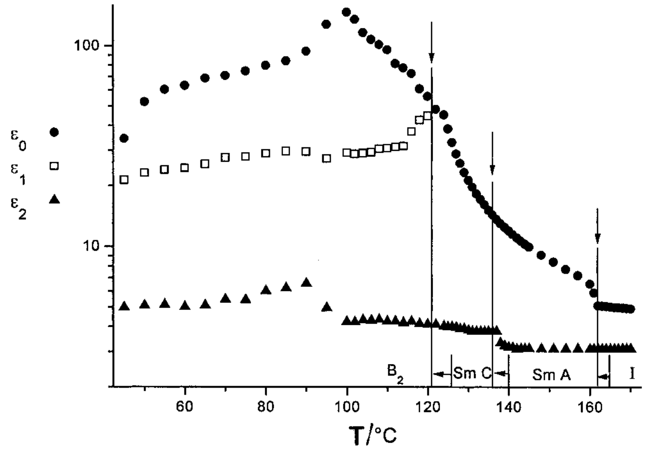

Figure 5. Fitted dielectric constants according to the Cole–Cole equation. The horizontal arrows indicate the shift of phase transition temperatures which is due to partial decomposition of the substance at high temperatures.

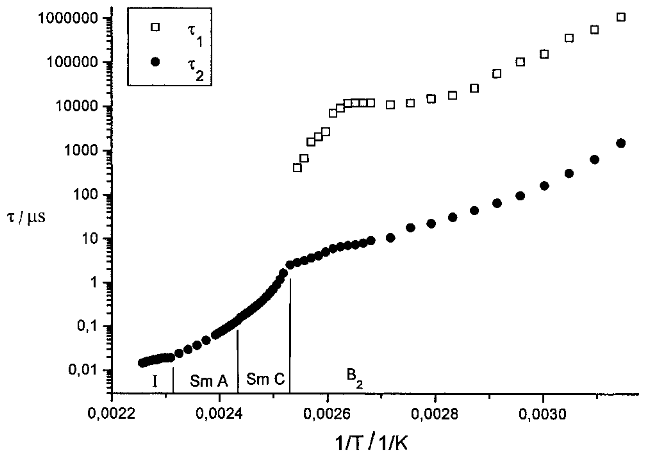

Figure 6. Fitted dielectric relaxation times according to the Cole–Cole equation.

X-ray Measurements for non-oriented samples indicate a layer structure without in-plane order for the three mesophases described above. Figure 7 displays the scattering diagram of the B_2 phase in the small and wide angle regions. It is identical to that of the SmC phase, as expected for these phases, but it clearly rules out the existence of other smectic phases like higher ordered phases or Sm$\tilde{C}$ phases. In connection with the switching behaviour and the dielectric processes, the results strongly support the existence of the B_2 phase. The layer period (*d*-value) however displays a quite unusual behaviour. Instead of an expected decrease with decreasing temperature, the layer spacing increases slightly and continuously at the transitions SmA → SmC and SmC → B_2 (see figure 8). The *d*-value in the B_2 phase was found to be 5.1 nm (in comparison the length of the bent molecule is about 6 nm).

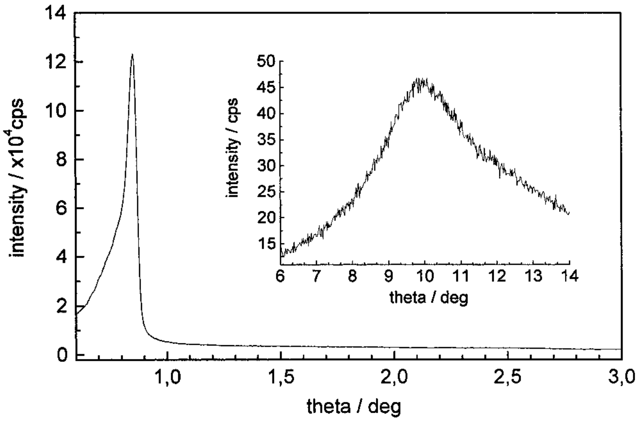

Figure 7. Scattering diagrams of the B_2 phase (T = 100°C). The small angle region has been measured with the small angle equipment. The scattering in the wide angle region has been recorded with a Guinier goniometer.

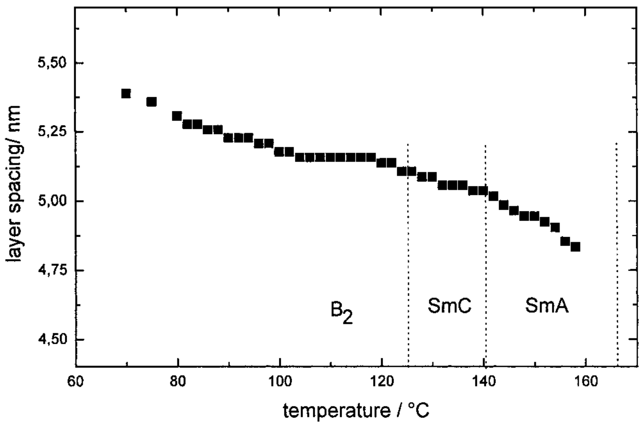

Figure 8. Temperature dependence of the layer spacing *d* in the SmA, SmC and B_2 phase.

These data point to a non-conventional packing of the molecules probably connected with different molecular conformations in the different mesophases. Up to now oriented samples have not been available. Such investigations together with NMR measurements will be the subject of a forthcoming paper using further alkyl and alkyloxy derivatives of the same class of substance.

References

[1] Niori, T., Sekine, T., Watanabe, J., Furukawa, T., and Takezoe, H., 1996, *J. mater. Chem.*, **6,** 1231.

[2] Pelzl, G., Diele, S., and Weissflog, W., 1999, *Adv. Mater.*, **11,** 707.

[3] Sekine, T., Niori, T., Sone, M., Watanabe, J., Choi, S. W., Takanashi, Y., and Takezoe, H., 1997, *Jpn. J. appl. Phys.*, **36,** 6455.

[4] Heppke, G., Krüerke, D., Löhning, C., Lötzsch, D., Rauch, S., and Sharma, N. K., 1997, Freiburger Arbeitstagung Flüssigkristalle, Poster P70.

[5] Diele, S., Grande, S., Kruth, H., Lischka, Ch., Pelzl, G., Weissflog, W., and Wirth, I., 1998, *Ferroelectrics*, **212,** 169.

[6] Pelzl, G., Diele, S., Jakli, A., Lischka, Ch., Wirth, I., and Weissflog, W., 1999, *Liq. Cryst.*, **26,** 135.

[7] Pelzl, G., Diele, S., Grande, S., Jakli, A., Lischka, Ch., Kresse, H., Schmalfuss, H., Wirth, I., and Weissflog, W., 1999, *Liq. Cryst.*, **26,** 401.

[8] Weissflog, W., Lischka, Ch., Diele, S., Pelzl, G., and Wirth, I., 1999, *Mol. Cryst. liq. Cryst.*, **328,** 101.

[9] Bedel, J. P., Nguyen, H. T., Rouillon, R. C., Marcerou, J. P., Sigaud, G., and Barois, P., 1999, *Mol. Cryst. liq. Cryst.*, **332,** 163.

[10] Nguyen, H. T., Rouillon, J. C., Marcerou, J. P., Bedel, J. P., Barois, P., and Sarmento, S., 1999, *Mol. Cryst. liq. Cryst.*, **328,** 177.

[11] Heppke, G., Parghi, D. D., and Sawade, H., 1999, Freiburger Arbeitstagung Flüssigkristalle, Poster P42.

[12] Shen, D., Diele, S., Pelzl, G., Wirth, I., and Tschierske, C., 1999, *J. mater. Chem.*, **9,** 661.

[13] Shen, D., Diele, S., Wirth, I., and Tschierske, C., 1998, *Chem. Commun.*, 2573.

[14] Lee, C.-W., and Chien, L.-C., 1999, *Liq. Cryst.*, **26,** 609.

[15] Diele, S., Pelzl, G., and Weissflog, W., 1999, *Liq. Cryst. Today*, **9,** 8.

[16] Marcus, E., 1891, *Chem. Ber.*, **24,** 3650.

[17] Serrano, J. L., Sierra, T., Gonzalez, Y., Bolm, C., Weickardt, K., Magnus, A., and Moll, G., 1995, *J. Am. chem. Soc.*, **117,** 8312.

[18] Weissflog, W., Lischka, Ch., Diele, S., Pelzl, G., Wirth, I., Grande, S., Kresse, H., Schmalfuss, H., Hartung, H., and Stettler, A., 1999, *Mol. Cryst. liq. Cryst.*, **333,** 203.

[19] Schmalfuss, H., Shen, D., Tschierske, C., and Kresse, H., 1999, *Liq. Cryst.*, **26,** 1767.

[20] Hauser, A., Schmalfuss, H., and Kresse, H., *Liq. Cryst.* (in the press).